Nonlinear Dynamics of Paced Cardiac Cells

YOHANNES SHIFERAW,[a] ZHILIN QU,[a] ALAN GARFINKEL,[a] ALAIN KARMA,[b] AND JAMES N. WEISS[a,c]

[a]*Department of Medicine (Cardiology), David Geffen School of Medicine at UCLA, Los Angeles, California 90095, USA*

[b]*Department of Physics and Center for Interdisciplinary Research on Complex Systems, Northeastern University, Boston, Massachusetts 02115, USA*

[c]*Department of Physiology, David Geffen School of Medicine at UCLA, Los Angeles, California 90095, USA*

ABSTRACT: When a cardiac cell is rapidly paced it can exhibit a beat-to-beat alternation in the action potential duration (APD) and the intracellular calcium transient. This dynamical instability at the cellular level has been shown to correlate with the genesis of cardiac arrhythmias and has motivated the application of nonlinear dynamics in cardiology. In this article, we review mathematical approaches to describe the underlying mechanisms for alternans using beat-to-beat iterated maps. We explain the development and properties of these maps, and show that they provide a fruitful framework to understand dynamical instabilities of voltage and calcium in paced cardiac cells.

KEYWORDS: nonlinear dynamics; alternans; calcium cycling; cardiac arrhythmias

INTRODUCTION

Ventricular fibrillation (VF) occurs when electrical waves in the heart breaks up into multiple wavelets. This breakup has been traditionally attributed to the presence of fixed anatomical and/or electrophysiological heterogeneities in the heart, such as the presence of an infraction or ischemic zone. However, recent experimental and theoretical studies have shown that the dynamical properties of cardiac cells can play an important role in promoting VF.[1,2] In this case, it is argued that the onset and maintenance VF is dictated by the intrinsic dynamics of cardiac cells, such as the gating kinetics of ion channels. From this perspective, it is critical to explore the dynamical behavior of cardiac cells in order to fully understand the genesis and maintenance of VF.

Address for correspondence: James N. Weiss, Division of Cardiology, 3645 MRL Building, David Geffen School of Medicine at UCLA, Los Angeles, CA 90095. Voice: 310-825-9029; fax: 310-206-5777.
e-mail: jweiss@mednet.ucla.edu

Ann. N.Y. Acad. Sci. 1080: 376–394 (2006).
doi: 10.1196/annals.1380.028.x

The relationship between the dynamics of cardiac cells and arrhythmogenesis at the whole heart level has been studied extensively in the last decade.[1–4] Much of this work has centered around the experimentally observed phenomenon of "alternans,"[5,6] where the action potential duration (APD) and calcium transient alternate from one beat to the next. Alternans occurs during rapid pacing or pathophysiological conditions, such as ischemia and heart failure. The observation of alternans in a clinical setting has been shown to correlate with sudden cardiac death.[7–10] Alternans has also been studied theoretically as a period doubling instability of rapidly paced cardiac cells which can induce the break up of reentrant activity in the heart.[1,2] These studies and others have highlighted the intimate connection between nonlinear dynamics at the cellular level, and the genesis of cardiac arrhythmias in the heart.

In this article we give an overview of recent experimental and theoretical work on the nonlinear dynamical properties of paced cardiac cells. After reviewing the experimental literature on both calcium transient and APD alternans, we describe theoretical approaches to explain this phenomenon using iterated nonlinear maps and physiologically based ionic models. In particular, we describe recent work on the nonlinear dynamics of calcium cycling in paced cardiac cells, and the rich dynamical behavior that arises due to the bidirectional coupling between membrane voltage dynamics and intracellular calcium.

ALTERNANS IN CARDIAC MYOCYTES: EXPERIMENTAL OBSERVATIONS

APD alternans has been observed in a wide variety of cardiac cell types and experimental conditions (see Refs. 5 and 6 for comprehensive reviews of the experimental literature). Experimentally, APD alternans is typically observed during rapid pacing at fixed pacing frequency, as shown in FIGURE 1 A, so that beyond a critical pacing frequency the normally periodic response is replaced by a sequence of long and short APDs. If the rapid pacing frequency is held fixed, then this alternating pattern is maintained at steady state. This is in contrast to transient alternans which occurs for only several beats immediately after an abrupt change in pacing frequency. APD alternans has also been observed when a cardiac cell is paced after pharmacologic or other interventions. For example, application of tetracaine[11] and pyruvate[12] are known to induce alternans in cardiac cells. Also APD alternans has been observed at low pacing rates under ischemic conditions.[12]

Fluorescence imaging of intracellular calcium reveals that the calcium transient can also alternate from beat to beat.[5,13,14] In this case, the peak of the calcium transient, which measures the amount of calcium released during one beat from the sarcoplasmic reticulum (SR) to the bulk myoplasm, typically alternates in a large-small-large sequence. Again, this pattern can be observed

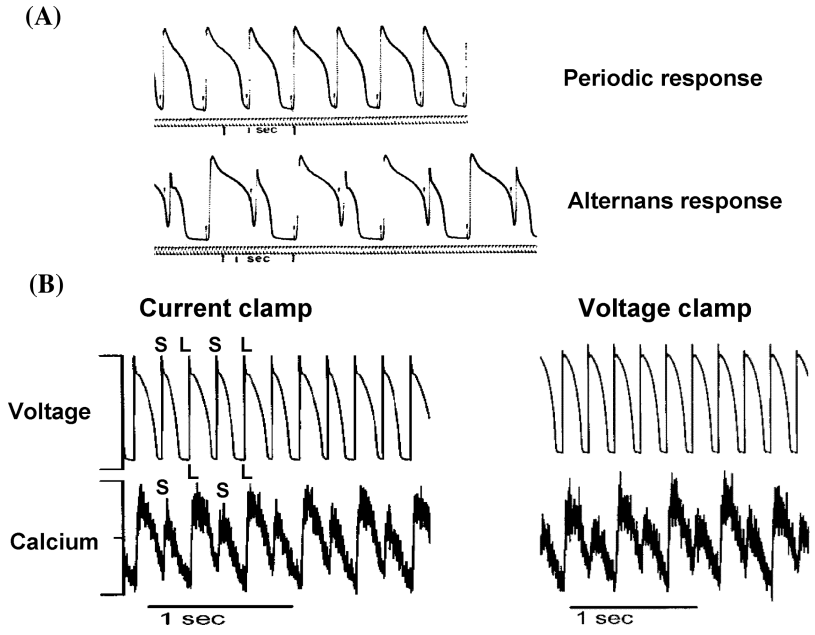

FIGURE 1. Experimental observations of APD and calcium-transient alternans in paced cardiac cells. (**A**) Periodic and alternans response measured in frog ventricular muscle strips, as observed in Nolasco and Dahlen's classic study.[16] (**B**) APD and calcium-transient alternans observed under current and AP clamp conditions in rabbit ventricular myocytes.[14] As shown, alternans in the calcium-transient was still observed when the membrane voltage was clamped using a periodic AP waveform.

at steady state, and also as a transient response to a change in pacing cycle length. Experimentalists have also recorded APD alternans simultaneously with calcium-transient alternans (see FIG. 1 B), or alternatively, cell contraction, which is known to be directly proportional to the peak of the calcium transient. In these measurements, alternans in the calcium transient (contraction) is always associated with alternans of APD. This is not surprising because intracellular calcium and membrane voltage are bidirectionally coupled via calcium-sensitive ion currents that regulate voltage. Moreover, the features of this bidirectional coupling are dependent on species and experimental conditions. For example, in rabbit heart ventricular cells, a large-small-large calcium transient is typically associated with a long-short-long APD[14] (electromechanically in-phase), while in cat atrial cells a large-small-large calcium corresponds to a short-long-short APD[12] (electromechanically out-of-phase). Both of these dynamical modes have been observed in a variety of species and experimental conditions,[5] revealing the underlying complexity of the system.

In critical experiments, Chudin *et al.*[14] paced a rabbit ventricular cell under both current and AP clamp conditions. As shown in FIGURE 1 B, they found

that under current clamp conditions, both the APD and the calcium transient alternated in-phase. However, when the AP was clamped using a periodic waveform, as shown in FIGURE 1 C, they found that calcium-transient alternans still occurred. This result demonstrated convincingly that calcium alternans, at least in the rabbit, can originate from a dynamical instability of calcium cycling, independently of APD alternans. Diaz *et al.*[15] paced rat ventricular myocytes using a square voltage clamp waveform and showed that they could induce a form of alternans in which every other beat was associated with a propagating intracellular calcium wave. Again, this result showed that alternans originated via a mechanism intrinsic to the calcium cycling machinery, and independently of the dynamics of membrane voltage.

ALTERNANS AND APD RESTITUTION

The first theoretical explanation of APD alternans is attributed to Nolasco and Dahlen[16] who pioneered a geometrical construction, equivalent to iterating a discrete map, to elucidate the mechanism of APD alternans. Their basic assumption was that the APD at any given beat was completely determined by the time spent at full repolarization at the previous beat, that is, the diastolic interval (DI). This assumption was motivated by the basic observation that changes in the APD always correlated with changes in DI, and the intuitive notion that the APD should depend on recovery processes which occur during the previous DI. The corresponding map that describes beat-to-beat changes of APD is given by

$$APD_{n+1} = F(DI_n), \tag{1}$$

where APD_{n+1} is the APD measured for the $n+1th$ beat, and DI_n is the DI at the previous beat. This functional relationship is referred to as the restitution curve. Nolasco and Dahlen showed geometrically that if the cell is paced at a pacing period $T = APD^* + DI^*$, such that

$$\left.\frac{dF}{dDI_n}\right|_{DI_n = DI^*} > 1, \tag{2}$$

where DI^* denotes the steady state DI, then a beat-to-beat alternation of the APD would ensue. Thus, alternans would arise when the slope of the restitution curve is steep, and small changes in DI lead to large variations of APD during the ensuing beat. Later Guevarra *et al.*[17,18] cast the Nolasco and Dahlen analysis in the mathematical language of nonlinear dynamics, and identified alternans as a period doubling bifurcation of the nonlinear mapping given by Equation 1.

Beyond the discrete map approach, alternans can also be studied by modeling the dynamics of membrane voltage using the standard equation

$$\frac{dV}{dt} = -\frac{1}{C_m}(I_{ion} + I_{stim}), \quad \textbf{(3)}$$

where C_m is the cell membrane capacitance, I_{ion} is the current due to Na^+, K^+, Ca^{2+} ions flowing across the membrane, and where I_{stim} is a periodically applied stimulus current. Much work has been devoted to developing physiologically accurate models for I_{ion} , by fitting the kinetic properties of measured ion currents and incorporating these formulations in Hodgkin–Huxley type ordinary differential equations (ODEs).[18–25] Using this approach, alternans can be obtained during steady state pacing if the kinetics of ion currents are adjusted appropriately. For instance Qu *et al.*[26] used the first generation Luo-Rudy model[27] to show that alternans can be obtained at rapid rates when the time constant of the slow outward current was adjusted to steepen the APD restitution curve. Also, Karma[1,28] analyzed alternans in a model of Purkinje cells due to Noble,[29] and showed that alternans onset was determined by the slope of the restitution curve. Finally, Fenton and Karma[30] obtained APD alternans at high rates using a simplified three-variable ionic model. In all these models the restitution relationship (Equation 1) computed using the ionic model was found to be correct. That is, the APD was essentially determined by the previous DI, and alternans were observed precisely when the slope of the restitution curve exceeded 1.

In an experimental setting, the APD restitution curve has traditionally been measured using the S1-S2 restitution protocol, where the cell is paced to steady state at a pacing interval S1, before applying an extrastimulus at a pacing interval S2, as illustrated in FIGURE 2 A. The APD of the S2 beat is then measured and graphed with respect to the previous DI. Several experimental studies have attempted to uncover the ionic mechanisms that regulate the APD restitution curve. An older study in mammalian myocardial fibers by Gettes and

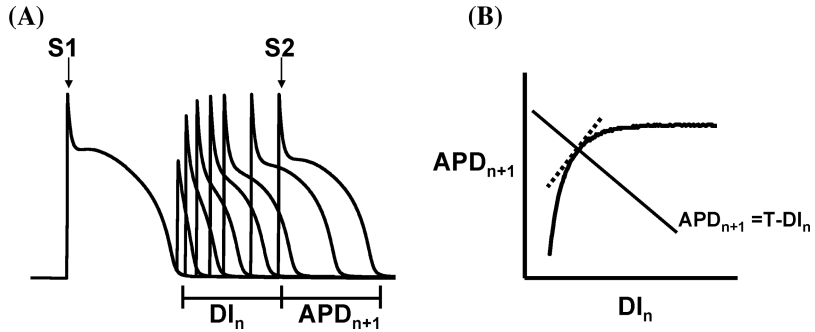

FIGURE 2. The APD restitution curve and alternans. (**A**) Demonstration of the measurement of the APD restitution curve using the S1-S2 protocol. (**B**) APD restitution curve showing intersection with the line $APD_{n+1} = T\text{-}DI_n$ where T is the pacing period. The dashed line represents the slope which controls the onset of steady state APD alternans.

Reuter[31] showed that recovery from inactivation of the L-type calcium current was the dominant factor in dictating the shape of the APD restitution curve. More recently, Goldhaber *et al.*[32] showed in rabbit ventricular myocytes that the steepness of the restitution curve measured at physiological temperatures was strongly dependent on the time course of recovery of the L-type calcium current. Other studies[33–35] have also shown that incomplete deactivation of K^+ currents can substantially influence the shape of the APD restitution curve. A comprehensive analysis of ion currents in the ferret ventricular cells due to Janvier *et al.*,[36] showed that the sodium–calcium exchange current (I_{NaCa}) and the fast outward K^+ current (I_{to}) were also critical in shaping the AP. Thus, in general a variety of ionic mechanisms contribute to the shape of the APD restitution curve.

The connection between alternans and the shape of the restitution curve has been investigated experimentally. Saitoh *et al.*[37] applied different doses of lidocaine to modulate the slope of the APD restitution curve in dog Purkinje muscle fibers. They found that the magnitude of APD alternans, measured after a change in cycle length, increased in proportion to the slope of the APD restitution curve. Further work by Riccio *et al.*[38] in the canine hearts showed that drugs which selectively flattened the APD restitution curve, such as procainamide and verapamil, abolished alternans. These results showed convincingly that the restitution slope has a major influence on the dynamics of alternans.

LIMITATIONS OF THE RESTITUTION HYPOTHESIS

The APD restitution relationship is an essential tool to understand the dynamics of alternans in paced cardiac cells. However, in many experiments, Equation 2 does not hold precisely. That is, the restitution relationship does not always predict the precise onset of alternans. For example Hall *et al.*[39] found that alternans was absent even though the slope of the APD restitution curve significantly exceeded 1. Also, in a comprehensive study, Dilly and Lab[40] found that during ischemia, alternans was observed even though the restitution slope was significantly less than 1. More recent work in the guinea pig heart[41] showed that the onset of alternans in the epicardium did not correlate with regions where the APD restitution curve was the steepest. These results indicate that in many cases the APD restitution curve may not give a complete quantitative description of alternans dynamics.

A major shortcoming of the APD restitution relationship is that it assumes that the APD is dependent only on the previous DI. Or rather, in the language of ion current kinetics, that the ionic recovery processes that occur during the DI completely determine the ensuing APD. However, this picture is clearly over simplified. First, ionic recovery processes that occur during times before the previous DI may also influence, to some degree, the APD at a later beat.

Second, the ionic concentrations in the cell can accumulate as a function of pacing rate via the dynamics of the various ion pumps and exchangers which determine the steady state properties. This ion accumulation can occur over many beats and is distinct from gating kinetics which typically have a much shorter time scale. A direct consequence of these factors is that the APD is likely to depend on the pacing history of the cell, an effect referred to in the literature as "cardiac memory" or "APD accommodation."[42–44]

In the experimental setting, this effect is manifested in the fact that the APD restitution curve can only be defined once the pacing history of the cell has been specified. For instance, a dynamic APD restitution curve can also be defined,[38] where the cell is paced to steady state at a fixed pacing interval, and the steady state APD and DI are recorded. A sequence of pacing intervals are scanned and the steady state APDs are then graphed with respect to the steady state DIs. Note that if the restitution relationship given in Equation 1 holds exactly, then the curve measured using the dynamic and S1-S2 protocols should be the same. However, in general these curves can be quite different. For example, Elharrar and Surawicz[45] found that the S1-S2 restitution curve in dog cardiac fibers depended critically on the S1 interval chosen, and was significantly steeper than the dynamic restitution curve at small DIs, while much shallower at larger DIs. On the other hand, measurements in the canine ventricle[38] showed that the S1-S2 restitution was significantly flatter than the dynamic restitution curve. These authors also found that alternans were observed in these hearts when the dynamic restitution slope was greater than 1, while the S1-S2 restitution slope was less than 1. These results suggest that in the canine ventricle the dynamic restitution curve is more predictive of alternans.

In order to model the effect of memory, Tolkacheva *et al.*[46] have attempted to generalize the restitution relationship in order to obtain a more accurate determinant of the onset of alternans. As a starting point they replaced the restitution relationship given in Equation 1 with

$$APD_{n+1} = F(DI_n, APD_n), \tag{4}$$

so that the APD depends on both the previous DI and APD. Given this map, they showed that indeed the slope of the dynamic restitution curve (S_{dyn}) was not the same as the S1-S2 restitution slope (S_{S1S2}), and also that the onset of alternans was instead given by the condition,

$$\left| 1 - \left(1 + \frac{1}{S_{dyn}} \right) S_{S1S2} \right| > 1. \tag{5}$$

Given this relation, it is easy to see that simply measuring S_{S1S2}or S_{dyn} alone is not enough to determine the onset of alternans. These authors have also considered more general relationships[47] of the form

$$APD_{n+1} = F(DI_n, APD_n, DI_{n-1}, APD_{n-1}, \ldots), \tag{6}$$

and have developed a hierarchy of restitution protocols which can be used to more precisely predict the onset of alternans. However, experimental validation of these results has not yet been achieved. These, and other results,[43,44] show that further work is required in order to construct more quantitative discrete maps which can be used to more accurately predict alternans dynamics.

CALCIUM CYCLING AND ALTERNANS

The experimental and theoretical studies mentioned above suggest that the APD restitution relationship given by Equation 1 is too restrictive and that memory effects have to be taken into account for a more complete description of alternans. However, these modifications are still made under the assumption that the APD is completely determined by the history of the membrane voltage of the cell. However, this basic assumption will not be true if voltage is coupled to dynamical processes inside the cell which have their own intrinsic dynamics. This possibility is borne out in the experiments of Chudin *et al.*[14] who showed that calcium-transient alternans can be observed even though the cell was paced with a periodic voltage clamp. Hence, in order to completely understand the dynamics of alternans in cardiac cells it is crucial to understand the nonlinear dynamics of calcium cycling.

During an AP, calcium is released from intracellular stores and signals cell contraction.[48,49] Several mathematical models have been proposed to describe the dynamics of calcium cycling.[21,22,50–52] However, a fundamental difficulty, often overlooked in modeling studies, is that calcium release is a local process which occurs within several thousand submicron scale junctions distributed throughout the volume of the cell. Within these junctions, localized clusters of calcium release channels called ryanodine receptors (RyR), which gate the flow of calcium from intracellular stores into the cytoplasm, open in response to calcium entry via L-type calcium channels on the surface cell membrane.[48] Signaling within these junctions occurs via a calcium-induced calcium-release (CICR) process which endows the calcium system with a rich dynamical behavior (see FIG. 3 for an illustration of the calcium cycling system). In a classic theoretical study, Stern[53] pointed out that basic features of excitation–contraction (EC) coupling in cardiac cells, such as the roughly linear relation between calcium entry and release, cannot be explained without explicitly accounting for the local nature of calcium signaling in the cell.

In order to resolve these difficulties Shiferaw *et al.*[52] introduced a phenomenological model of calcium cycling which explicitly accounted for the local nature of calcium release. Using this model, calcium-transient alternans could be induced at rapid pacing rates when the cell was paced with a periodic AP clamp. A mathematical reduction of the ODEs describing calcium cycling revealed that close to the periodic fixed point the beat-to-beat dynamics could

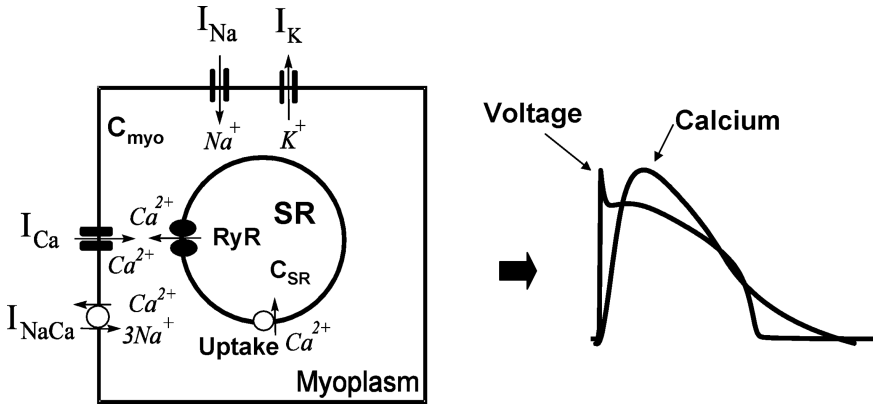

FIGURE 3. Illustration of calcium cycling machinery and membrane voltage currents. During calcium cycling calcium is released from the SR into the myoplasm, and then gets pumped back in to the SR via uptake pumps. Calcium release is triggered by the L-type calcium current via a CICR mechanism. Coupling between membrane voltage and intracellular calcium cycling is mediated by the L-type calcium current and the electrogenic sodium–calcium exchange current.

be reduced to a discrete mapping of calcium concentration variables in the SR and the myoplasm. This discrete mapping can be expressed as

$$c_{myo}^{n+1} = c_{myo}^{n} + R_n - U_n + \Delta_n, \tag{7}$$

$$c_{SR}^{n+1} = c_{SR}^{n} - R_n + U_n, \tag{8}$$

where c_{myo}^{n} and c_{SR}^{n} are the calcium concentration in the myoplasm and SR at the beginning of beat n (see FIG. 6 A for illustration of variables), R_n is the total amount of calcium released from the SR to the myoplasm during beat n, where U_n is the net amount of calcium pumped back into the SR during this beat (i.e., SR uptake less SR leak), and finally where Δ_n denotes the net calcium influx across the sarcolemma. Here, R_n, U_n, and Δ_n are functions of c_{SR}^{n} and c_{myo}^{n}, which can be explicitly computed from the ionic currents in the cell that participate in calcium cycling. Using this two-dimensional nonlinear mapping, which can be further reduced to one dimension by assuming that the total number of calcium ions in the cell is essentially constant from beat to beat, it is straightforward to show that calcium cycling is unstable to alternans when

$$-1 - \frac{\partial G_n}{\partial c_{myo}^{n}} + \frac{\partial G_n}{\partial c_{SR}^{n}} > 1, \tag{9}$$

where $G_n = R_n - U_n$. This relation reveals that calcium alternans can arise if the function G varies sufficiently steeply with respect to the SR load and/or the diastolic calcium concentration in the cell. In this sense, the function G_n

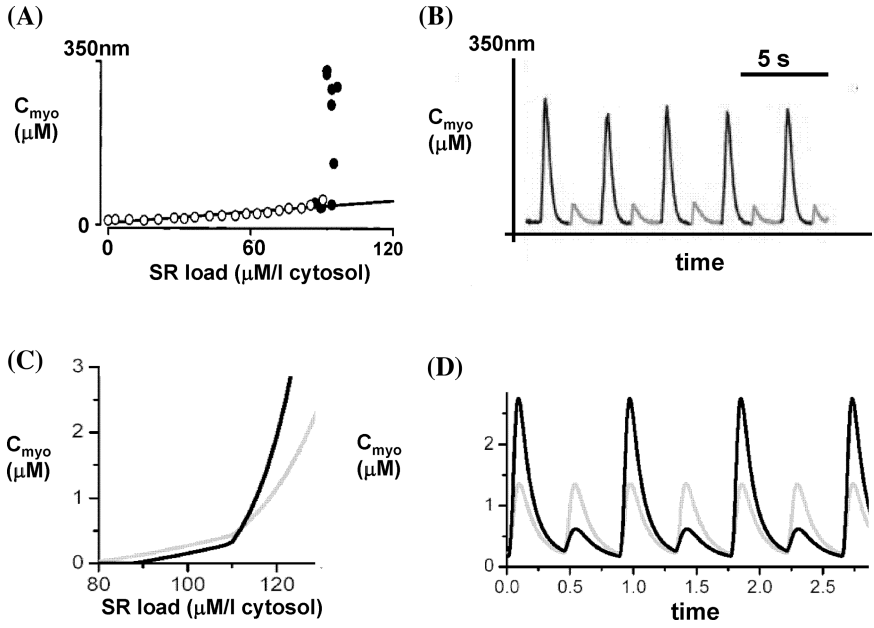

FIGURE 4. Demonstration of calcium-transient alternans in rat ventricular myocytes reproduced from Diaz *et al*.,[15] and also using a physiologically based mathematical model. (**A**) Experimental demonstration of a steep release-load functional relationship. Here, the peak of the calcium transient is plotted with respect to the SR load, which is estimated by integrating the sodium–calcium exchange current. (**B**) Calcium transients estimated by measuring the mean fluorescence in the cell. (**C**) Plot of peak calcium transient versus SR calcium load using the calcium cycling model of Shiferaw *et al.*[52] The dark/gray lines corresponds to a steep/shallow dependences of SR calcium release on SR load. (**D**) Alternans are observed when the release function is steep (dark traces), and not when it is shallow (gray traces).

controls the nonlinear dynamical properties of calcium cycling, in much the same way as the APD restitution function describes the dynamics of membrane voltage.

A recent experimental study due to Diaz e*t al.*[15] in the rat ventricular cells measured the SR calcium release as a function of the initial SR load. As shown in FIGURE 4 A and 4 B, which is reproduced from that study, they found that when the cell was paced using a square AP clamp, alternans were observed at high SR loads where the calcium released from the SR depended steeply on the SR load. Similarly, Shiferaw *et al.*[52] were able to induce alternans in their model by steepening the dependence of calcium release on SR calcium load, as shown in FIGURE 4 C and 4 D. Hence, as predicted by Equation 9, alternans can be induced by letting the calcium release process depend sensitively on the calcium concentration inside the SR. A possible explanation for this steep

dependence is that normally localized calcium release events may stimulate neighboring release units when the SR approaches a calcium overloaded state. This property will endow the release process with a nonlinear dependence of release on SR load which may drive alternans. A further analysis of the discrete mapping[52] revealed that the beat-to-beat dynamics can undergo even more complex dynamics, such as period 4, period 8, and chaotic dynamics if calcium released from the SR varied substantially with respect to the calcium concentration variables. These kinds of higher order periodicities have been frequently observed in paced cardiac cells,[43,44,54] and may be manifestations of chaotic properties of calcium cycling.

VOLTAGE AND CALCIUM DYNAMICS: TWO COUPLED NONLINEAR SYSTEMS

In the discussion so far, we have considered the nonlinear dynamics of membrane voltage independently of calcium cycling, and also of calcium cycling when driven with a clamped AP waveform. In general a complete understanding of alternans in cardiac myocytes will involve the coupled dynamics of both of these nonlinear systems. The dynamics of this coupled system is complex because it involves the interaction of ion channel kinetics which regulate the APD, and calcium fluxes which participate in the calcium cycling process. In this setting alternans can be induced via two independent mechanisms: (*a*) a steep dependence of APD on DI due to ionic recovery processes, that is, APD restitution, and (*b*) a steep calcium concentration dependence of calcium release and/or uptake between the SR and the myoplasm. Once alternans ensues by either of these mechanisms, both the APD and the calcium transient will alternate from beat to beat, because membrane voltage is bidirectionally coupled to intracellular calcium. Thus, in general it is difficult to pinpoint the underlying mechanism for alternans, especially in an experimental setting.

The essential feature of the system, which turns out to critically influence the coupled dynamics, is the precise nature of the bidirectional coupling between voltage and calcium. This coupling is mediated by calcium-sensitive ion currents, such as the L-type calcium current and the sodium–calcium exchange current (see FIG. 3), which mediate calcium cycling while also providing a substantial ionic flux across the cell membrane. Shiferaw *et al.*[55] identified several essential features of the bidirectional coupling which are critical to understanding the dynamics of the system. These are:

1. *Graded release coupling*: This involves the effect of the voltage waveform on the amount of calcium released from the SR, as illustrated in FIGURE 5 A. It is determined by the well-established phenomenon of graded SR calcium release,[48,56] where the amount of SR calcium released is graded with respect to the whole cell L-type calcium current. The availability of the L-type calcium current at a given beat depends critically on the previous DI, with larger

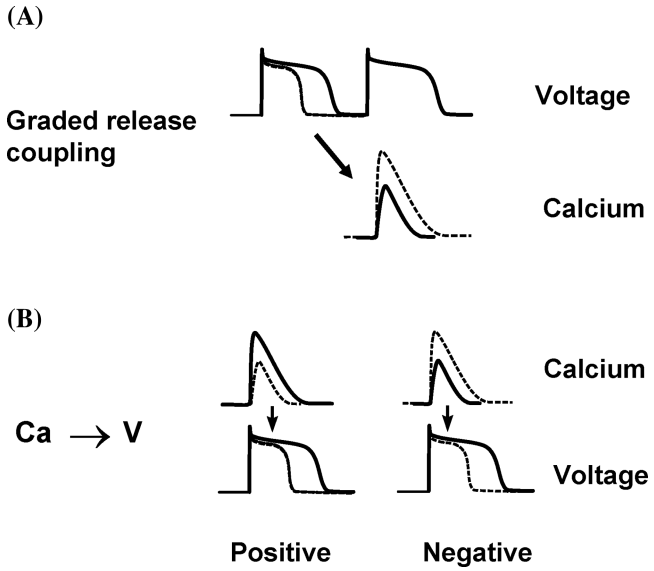

FIGURE 5. Illustration of bidirectional coupling between calcium and membrane voltage. (**A**) Graded release coupling between the APD and the calcium transient on the next beat. (**B**) Coupling between the calcium transient and the APD on the same beat. Positive/negative coupling denotes whether a larger calcium transient lengthens/shortens the APD.

DI giving more time for recovery of L-type calcium channels at the resting membrane potential. Thus, graded release requires that the peak of the calcium transient increases in response to an increase of DI in the previous beat.

2. *$Ca \rightarrow V$ coupling*: The coupling of the calcium transient on the APD, is illustrated in FIGURE 5 B. There are two parameter regimes which lead to distinct dynamical behaviors. The first, referred to as *positive $Ca \rightarrow V$ coupling,* corresponds to the case when a large peak calcium transient lengthens the APD of that beat. The second, referred to as *negative $Ca \rightarrow V$ coupling*, corresponds to the case when a large calcium transient shortens the APD. The sign of the coupling is dictated by the relative contributions of the L-type calcium current and the sodium–calcium exchange current to APD. A larger calcium transient tends to inactivate the whole cell L-type calcium current more rapidly via calcium-induced inactivation, which tends to shorten the APD. However, a large calcium transient also increases inward current from electrogenic sodium–calcium exchange, which tends to prolong APD.

Shiferaw *et al.*[55] studied the coupled dynamics of the system using a physiologically based ionic model due to Fox *et al.*[21] which was coupled to the

calcium cycling model described earlier. Using this model alternans could be induced by either steepening the dependence of calcium release on SR load, or alternatively, by increasing the time constant of recovery of the L-type calcium current to steepen the dependence of APD on DI. Shiferaw *et al.*[55] found that the dynamics of voltage and calcium alternans depended critically on both the underlying dynamical instability, and also on the sign of the $Ca \rightarrow V$ coupling. For *positive* $Ca \rightarrow V$ *coupling* calcium transient and APD alternans were always electromechanically in-phase, that is, a large-small-large calcium transient corresponds to long-short-long APD sequence. However, for *negative* $Ca \rightarrow V$ *coupling*, a much richer dynamical behavior was observed. In this case, if alternans is induced by unstable calcium cycling, then calcium and APD alternans are electromechanically out-of-phase, that is, a large-small-large calcium transient corresponds to a short-long-short APD sequence. On the other hand, if alternans is due to steep APD restitution, then calcium-transient alternans was in-phase with APD alternans. When both subsystems were unstable, both the calcium transient and APD exhibited quasi-periodic oscillations. Interestingly, the later dynamical mode has been observed experimentally in paced Purkinje fibers[43,44] and more recently in tissue cultures.[57]

In order to understand the qualitative nature of the coupled nonlinear dynamics, Shiferaw *et al.*[55] reduced their complex ionic model to a set of discrete maps that described the beat-to-beat evolution of voltage and calcium. The motivation was to integrate the classic restitution relationship given in Equation 1, with the nonlinear maps for calcium cycling given by Equations 7 and 8. In this case the beat-to-beat mapping of both calcium and APD can be described by a three-variable mapping of the form

$$\begin{aligned} APD_{n+1} &= F\left(DI_n, c^n_{myo}, c^n_{SR}\right) \\ c^{n+1}_{myo} &= c^n_{myo} + R_n - U_n + \Delta_n, \\ c^{n+1}_{SR} &= c^n_{SR} - R_n + U_n. \end{aligned} \tag{10}$$

Here, the first equation is simply a modification of the standard APD restitution relationship which includes the dependence of the APD on the diastolic calcium concentration c^n_{myo}, and the SR calcium load c^n_{SR}, as illustrated in FIGURE 6 A. Close to the onset of alternans, the total amount of calcium in the cell is roughly the same from beat to beat, so that the three-variable map can be reduced to a two-variable map. The condition for alternans can then be analyzed by computing the eigenvalues of the resulting two-dimensional discrete map. The condition for alternans is then given by the condition

$$\frac{1}{2}\left[\lambda_v + \lambda_c - \sqrt{(\lambda_v - \lambda_c)^2 + 4C}\right] > 1, \tag{11}$$

where

$$\lambda_v = \frac{\partial F}{\partial DI_n}, \tag{12}$$

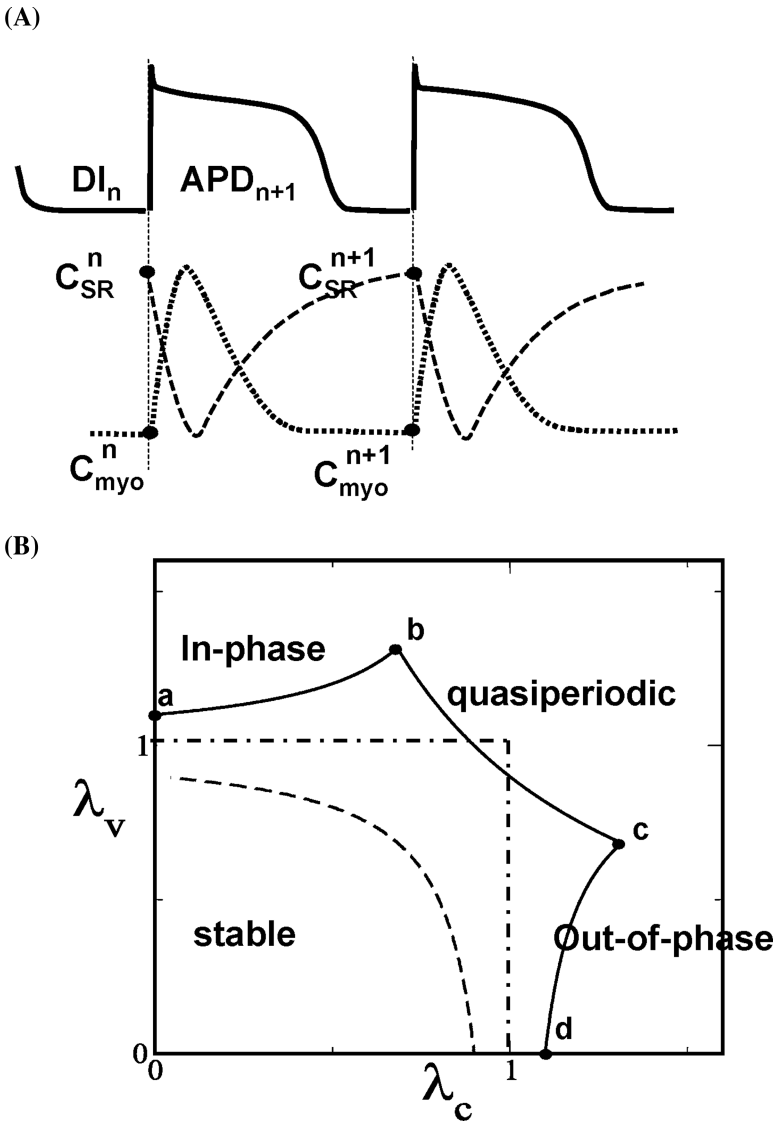

FIGURE 6. (**A**) Definition of discrete map variables describing the beat-to-beat dynamics of voltage and calcium. (**B**) Stability boundaries computed using the discrete map analysis. The dot-dashed lines denotes the stability boundary when voltage and calcium are uncoupled. The dashed line denotes the stability boundary when the $Ca \rightarrow V$ coupling is positive. In this case the periodic fixed point always looses stability to electromechanically in-phase alternans. The solid line denotes the stability boundary in the case of negative $Ca \rightarrow V$ coupling. Three dynamical modes are observed when the cell looses stability along the indicated line segments: electromechanically in-phase alternans (a–b), electromechanically out-of-phase alternans (c–d), and finally quasiperiodicity (b–c).

$$\lambda_c = -1 - \frac{\partial G}{\partial c^n_{myo}} + \frac{\partial G}{\partial c^n_{SR}}, \tag{13}$$

and where C is positive/negative depending on whether the $Ca \rightarrow V$ coupling is positive/negative. Here λ_v is simply the standard restitution slope, while λ_c measures the degree of instability of calcium cycling. For the case when voltage and calcium are uncoupled ($C = 0$), then Equation 11 simply reduces to Equation 2 and 9, found earlier by analyzing each system independently. In FIGURE 6 B, we plot Equation 11 to show the boundary separating stable periodic dynamics and unstable alternans or quasiperiodic dynamics. Now, when both systems are positively coupled ($C > 0$), the stability boundary is given by the dashed line. Here, we see that the domain of stability shrinks for positive coupling, showing that the coupled system is more unstable than its constituents, that is, APD alternans enhance calcium alternans and vice versa. On the other hand, when the coupling between calcium on voltage is negative ($C < 0$), then the stability boundary expands, so that the coupled system becomes more stable. In other words alternans in APD tends to stabilize calcium-transient alternans, and vice versa. Moreover, as seen in the ionic model simulations the fixed point can loose stability to electromechanically in-phase, out-of phase, and also a quasi-periodic dynamical mode.

The generalization of the standard APD restitution relationship to include calcium cycling, as given by the three-variable map in Equation 10, serves as a framework to interpret the rich set of dynamical behavior observed experimentally. The advantage of the map analysis is that it allows to interpret experiments in terms of three critical parameters: the APD restitution slope, the degree of instability of calcium cycling as measured by the concentration dependence of the release and uptake from the SR, and the sign of the calcium on voltage coupling. Remarkably, all three dynamical modes predicted by the model have been observed experimentally in different cell types and pharmacologic conditions,[5,6,43,44] and also in tissue cultures.[57] However, up to now these observations have not been explained within a general framework. It is interesting to speculate that perhaps these different cell types and pharmacologic interventions simply correspond to different points in the phase diagram shown in FIGURE 6 B.

SUMMARY

In this article we have reviewed the various mathematical approaches that have been applied to understand the nonlinear dynamics of paced cardiac cells. In particular, we have described the various theoretical approaches to describe alternans using discrete beat-to-beat maps. The main advantage of this approach is that it makes it possible to reduce the complex dynamics of a paced

cardiac cell to basic nonlinear relationships between experimentally measured quantities. Hence, this approach can help shed light on the key physiological mechanisms that underlie alternans, and help suggest experiments to uncover these mechanisms.

ACKNOWLEDGMENTS

This study was supported by NIH/NHLBI grant P01 HL078931, the Laubisch and Kawata endowments.

REFERENCES

1. KARMA, A. 1994. Electrical alternans and spiral wave breakup in cardiac tissue. Chaos **4:** 461–472.
2. GARFINKEL, A., Y.H. KIM, O. VOROSHILOVSKY, *et al*. 2000. Preventing ventricular fibrillation by flattening cardiac restitution. Proc. Natl. Acad. Sci. USA **97:** 6061–6066.
3. QU, Z. & A. GARFINKEL. 1999. An advanced algorithm for solving partial differential equation in cardiac conduction. IEEE Trans. Biomed. Eng. **46:** 1166–1168.
4. QU, Z., J.N. WEISS & A. GARFINKEL. 2000. From local to global spatiotemporal chaos in a cardiac tissue model. Phys. Rev. E Stat. Phys. Plasmas Fluids Relat. Interdiscip. Topics **61:** 727–732.
5. EULER, D.E. 1999. Cardiac alternans: mechanisms and pathophysiological significance. Cardiovasc. Res. **42:** 583–590.
6. WALKER, M.L. & D.S. ROSENBAUM. 2003. Repolarization alternans: implications for the mechanism and prevention of sudden cardiac death. Cardiovasc. Res. **57:** 599–614.
7. PASTORE, J.M., S.D. GIROUARD, K.R. LAURITA, *et al*. 1999. Mechanism linking T-wave alternans to the genesis of cardiac fibrillation. Circulation **99:** 1385–1394.
8. PRUVOT, E.J. & D.S. ROSENBAUM. 2003. T-wave alternans for risk stratification and prevention of sudden cardiac death. Curr. Cardiol. Rep. **5:** 350–357.
9. ROSENBAUM, D.S., L.E. JACKSON, J.M. SMITH, *et al*. 1994. Electrical alternans and vulnerability to ventricular arrhythmias. N. Engl. J. Med. **330:** 235–241.
10. ARMOUNDAS, A.A., M. OSAKA, T. MELA, *et al*. 1998. T-wave alternans and dispersion of the QT interval as risk stratification markers in patients susceptible to sustained ventricular arrhythmias. Am. J. Cardiol. **82:** 1127–1129, A9.
11. DIAZ, M.E., D.A. EISNER & S.C. O'NEILL. 2002. Depressed ryanodine receptor activity increases variability and duration of the systolic Ca2+ transient in rat ventricular myocytes. Circ. Res. **91:** 585–593.
12. HUSER, J., Y.G. WANG, K.A. SHEEHAN, *et al*. 2000. Functional coupling between glycolysis and excitation-contraction coupling underlies alternans in cat heart cells. J. Physiol. **524:** 795–806.
13. EISNER, D.A., H.S. CHOI, M.E. DIAZ, *et al*. 2000. Integrative analysis of calcium cycling in cardiac muscle. Circ. Res. **87:** 1087–1094.
14. CHUDIN, E., J. GOLDHABER, A. GARFINKEL, *et al*. 1999. Intracellular Ca(2+) dynamics and the stability of ventricular tachycardia. Biophys. J. **77:** 2930–2941.

15. DIAZ, M.E., S.C. O'NEILL & D.A. EISNER. 2004. Sarcoplasmic reticulum calcium content fluctuation is the key to cardiac alternans. Circ. Res. **94:** 650–656.
16. NOLASCO, J.B. & R.W. DAHLEN. 1968. A graphic method for the study of alternation in cardiac action potentials. J. Appl. Physiol. **25:** 191–196.
17. GUEVARA, M.R., L. GLASS & A. SHRIER. 1981. Phase locking, period-doubling bifurcations, and irregular dynamics in periodically stimulated cardiac cells. Science **214:** 1350–1353.
18. GUEVARA, M.R., G. WARD, A. SHRIER & L. GLASS. 1984. Electrical alternans and period doubling bifurcations. IEEE Comput. Cardiol. 167–170.
19. BEELER, G.W. & H. REUTER. 1977. Reconstruction of the action potential of ventricular myocardial fibres. J. Physiol. **268:** 177–210.
20. LUO, C.H. & Y. RUDY. 1994. A dynamic model of the cardiac ventricular action potential. I. Simulations of ionic currents and concentration changes. Circ. Res. **74:** 1071–1096.
21. FOX, J.J., J.L. MCHARG & R.F. GILMOUR, JR. 2002. Ionic mechanism of electrical alternans. Am. J. Physiol. Heart Circ. Physiol. **282:** H516–H530.
22. JAFRI, M.S., J.J. RICE & R.L. WINSLOW. 1998. Cardiac Ca2+ dynamics: the roles of ryanodine receptor adaptation and sarcoplasmic reticulum load. Biophys. J. **74:** 1149–1168.
23. RICE, J.J., M.S. JAFRI & R.L. WINSLOW. 1999. Modeling gain and gradedness of Ca2+ release in the functional unit of the cardiac diadic space. Biophys. J. **77:** 1871–1884.
24. BONDARENKO, V.E., G.P. SZIGETI, G.C. BETT, *et al*. 2004. Computer model of action potential of mouse ventricular myocytes. Am. J. Physiol. Heart Circ. Physiol. **287:** H1378–H1403.
25. BONDARENKO, V.E., G.C. BETT & R.L. RASMUSSON. 2004. A model of graded calcium release and L-type Ca2+ channel inactivation in cardiac muscle. Am. J. Physiol. Heart Circ. Physiol. **286:** H1154–H1169.
26. QU, Z., J.N. WEISS & A. GARFINKEL. 1999. Cardiac electrical restitution properties and stability of reentrant spiral waves: a simulation study. Am. J. Physiol. **276:** H269–H283.
27. LUO, C.H. & Y. RUDY. 1991. A model of the ventricular cardiac action potential. Depolarization, repolarization, and their interaction. Circ. Res. **68:** 1501–1526.
28. KARMA, A. 1993. Spiral breakup in model equations of action potential propagation in cardiac tissue. Phys. Rev. Lett. **71:** 1103–1106.
29. NOBLE, D. 1962. A modification of the Hodgkin–Huxley equations applicable to Purkinje fibre action and pace-maker potentials. J. Physiol. **160:** 317–352.
30. FENTON, F. & A. KARMA. 1998. Vortex dynamics in three-dimensional continuous myocardium with fiber rotation: filament instability and fibrillation. Chaos **8:** 20–47.
31. GETTES, L.S. & H. REUTER. 1974. Slow recovery from inactivation of inward currents in mammalian myocardial fibres. J. Physiol. **240:** 703–724.
32. GOLDHABER, J.I., L.H. XIE, T. DUONG, *et al*. 2005. Action potential duration restitution and alternans in rabbit ventricular myocytes: the key role of intracellular calcium cycling. Circ. Res. **96:** 459–466.
33. DE HEMPTINNE, A. 1971. The frequency dependence of outward current in frog auricular fibres. An experimental and theoretical study. Pflugers Arch. **329:** 332–340.

34. HAUSWIRTH, O., D. NOBLE & R.W. TSIEN. 1972. Separation of the pace-maker and plateau components of delayed rectification in cardiac Purkinje fibres. J. Physiol. **225:** 211–235.
35. HUA, F. & R.F. GILMOUR, JR. 2004. Contribution of IKr to rate-dependent action potential dynamics in canine endocardium. Circ. Res. **94:** 810–819.
36. JANVIER, N.C., S.O. MCMORN, S.M. HARRISON, *et al*. 1997. The role of Na(+)-Ca2+ exchange current in electrical restitution in ferret ventricular cells. J. Physiol. **504:** 301–314.
37. SAITOH, H., J.C. BAILEY & B. SURAWICZ. 1989. Action potential duration alternans in dog Purkinje and ventricular muscle fibers. Further evidence in support of two different mechanisms. Circulation **80:** 1421–1431.
38. RICCIO, M.L., M.L. KOLLER & R.F. GILMOUR, JR. 1999. Electrical restitution and spatiotemporal organization during ventricular fibrillation. Circ. Res. **84:** 955–963.
39. HALL, G.M., S. BAHAR & D.J. GAUTHIER. 1999. Prevalence of rate-dependent behaviors in cardiac muscle. Phys. Rev. Lett. **82:** 2995.
40. DILLY, S.G. & M.J. LAB. 1988. Electrophysiological alternans and restitution during acute regional ischaemia in myocardium of anaesthetized pig. J. Physiol. **402:** 315–333.
41. PRUVOT, E.J., R.P. KATRA, D.S. ROSENBAUM & K.R. LAURITA. 2004. Role of calcium cycling versus restitution in the mechanism of repolarization alternans. Circ. Res. **94:** 1083–1090.
42. WATANABE, M.A. & M.L. KOLLER. 2002. Mathematical analysis of dynamics of cardiac memory and accommodation: theory and experiment. Am. J. Physiol. Heart Circ. Physiol. **282:** H1534–H1547.
43. GILMOUR, R.F., JR., N.F. OTANI & M.A. WATANABE. 1997. Memory and complex dynamics in cardiac Purkinje fibers. Am. J. Physiol. **272:** H1826–H1832.
44. OTANI, N.F. & R.F. GILMOUR, JR. 1997. Memory models for the electrical properties of local cardiac systems. J. Theor. Biol. **187:** 409–436.
45. ELHARRAR, V. & B. SURAWICZ. 1983. Cycle length effect on restitution of action potential duration in dog cardiac fibers. Am. J. Physiol. **244:** H782–H792.
46. TOLKACHEVA, E.G., D.G. SCHAEFFER, D.J. GAUTHIER & W. KRASSOWSKA. 2003. Condition for alternans and stability of the 1:1 response pattern in a "memory" model of paced cardiac dynamics. Phys. Rev. E Stat. Nonlin. Soft Matter Phys. **67:** 031904–031913.
47. KALB, S.S., E.G. TOLKACHEVA, D.G. SCHAEFFER, *et al*. 2005. Restitution in mapping models with an arbitrary amount of memory. Chaos **15:** 23701.
48. BERS, D.M. 2002. Cardiac excitation-contraction coupling. Nature **415:** 198–205.
49. BERS, D.M. 2001. Excitation-Contraction Coupling and Cardiac Contractile Force. Kluwer. Boston.
50. SHANNON, T.R., F. WANG, J. PUGLISI, *et al*. 2004. A mathematical treatment of integrated Ca dynamics within the ventricular myocyte. Biophys. J. **87:** 3351–331.
51. WINSLOW, R.L., J. RICE & S. JAFRI. 1998. Modeling the cellular basis of altered excitation-contraction coupling in heart failure. Prog. Biophys. Mol. Biol. **69:** 497–514.
52. SHIFERAW, Y., M.A. WATANABE, A. GARFINKEL, *et al*. 2003. Model of intracellular calcium cycling in ventricular myocytes. Biophys. J. **85:** 3666–3686.
53. STERN, M.D. 1992. Theory of excitation-contraction coupling in cardiac muscle. Biophys. J. **63:** 497–517.

54. CHIALVO, D.R., R.F. GILMOUR, JR. & J. JALIFE. 1990. Low dimensional chaos in cardiac tissue. Nature **343:** 653–657.
55. SHIFERAW, Y., D. SATO & A. KARMA. 2005. Coupled dynamics of voltage and calcium in paced cardiac cells. Phys. Rev. E Stat. Nonlin. Soft Matter Phys. **71:** 021903–021907.
56. WIER, W.G., T.M. EGAN, J.R. LOPEZ-LOPEZ & C.W. BALKE. 1994. Local control of excitation-contraction coupling in rat heart cells. J. Physiol. **474:** 463–471.
57. BIEN, H., L. YIN & E. ENTCHEVA. 2006. Calcium instabilities in mammalian cardiomyocyte networks. Biophys. J. **90:** 2628–2640.